Turkish Journal of Earth Sciences (Turkish J. Earth Sci.), **Vol. 10**, 2001, pp. 1-15. *Copyright ©TÜBİTAK*

Metamorphic and Tectonic Evolution of the Hırkadağ Block, Central Anatolian Crystalline Complex

DONNA L. WHITNEY[1] & YILDIRIM DİLEK[2]

[1] Department of Geology & Geophysics, University of Minnesota, Minneapolis, Minnesota, 55455 USA (e-mail: dwhitney@umn.edu)
[2] Department of Geology, Miami University, Oxford, Ohio, 45056 USA

Abstract: The Hırkadağ metamorphic block is a NE-SW-trending horst structure that is part of the Kırşehir Massif in the Central Anatolian Crystalline Complex (CACC). Along its southwestern margin, the block contains upper amphibolite facies metapelitic rocks that record peak metamorphic conditions of 670-710 °C, ~ 7 kbar, as determined by garnet-biotite geothermometry and garnet-sillimanite-plagioclase-quartz, garnet-rutile-sillimanite-ilmenite-quartz, and garnet-rutile-ilmenite-plagioclase-quartz geobarometry. A clockwise pressure-temperature path is inferred from thermobarometric results and analysis of reaction textures among aluminous phases. Following this medium-pressure metamorphism, low-pressure – high-temperature metamorphism resulted in widespread replacement of garnet by cordierite + spinel + sillimanite, partial replacement of spinel by corundum, and partial melting to produce granitic leucosomes. Garnet-cordierite thermobarometry indicates that low-P – high-T metamorphism occurred at 3 kbar, > 650 °C. This event may have occurred owing to isothermal decompression at high temperatures, or may have been related to magmatism, similar to intrusion-related low-P – high-T metamorphism elsewhere in the CACC.

High-angle normal faults bounding the southwestern and northeastern margins of the block truncate metamorphic structures and a granitic intrusion. These faults are part of a crustal-scale extension zone that uplifted the southern part of the Kırşehir Massif in the Late Tertiary, following its erosional exhumation in the Late Eocene.

Key Words: Central Anatolian Crystalline Complex, Hırkadağ, Kırşehir Massif, Metamorphism, Thermobarometry

Hırkadağ Bloğunun Metamorfik ve Tektonik Evrimi, Orta Anadolu Kristalen Kompleksi

Özet: KD-GB yönelimli bir horst yapısı gösteren Hırkadağ bloğu Orta Anadolu Kristalen Kompleksi içerisinde yer alan Kırşehir metamorfik masifinin bir parçasıdır. Hırkadağ bloğunun GB kesiminde yer alan metapelitik kayalar yüksek amfibolit derecesinde metamorfize olup, jeotermometrik ve jeobarometrik hesaplamalar sıcaklık ve basıncın 670-710 °C ve yaklaşık 7 kilobara kadar çıktığını göstermektedir. Termobarometrik hesaplamalar ve aluminyumlu mineral fazlarının gösterdiği reaksiyon dokularının özellikleri, Hırkadağ bloğunun genelde saat yönünde ilerleyen bir basınç-sıcaklık evrimi geçirdiğini ifade ederler. Bu orta basınç metamorfizmasını takiben, Hırkadağ metamorfitleri bir alçak basınç-yüksek sıcaklık metamorfizmasına uğramış olup, granatlar kordiyerit + spinel + sillimanite parajenezi, spinel ise korundum fazı tarafından replase edilmişlerdir. Aynı zamanda gelişen kısmi ergime de metamorfitler içerisinde yerleşen granitik sokulumlarını oluşturmuştur. Granat-kordiyerit termobarometrik hesaplamaları bu alçak basınç-yüksek sıcaklık metamorfizmasının yaklaşık 3 kilobarda ve 650 °C den yüksek sıcaklıklarda geliştiğini göstermektedir. Söz konusu alçak basınç-yüksek sıcaklık metamorfizması, Orta Anadolu Kristalen Kompleksi içerisindeki öteki masiflerde de gözlendiği gibi, çarpışma sonrası gelişen mağmatizma ile yakından ilişkilidir.

Hırkadağ bloğunu güneybatıdan ve kuzeydoğudan çevreleyen normal faylar aynı zamanda hem blok içerisindeki metamorfik yapıları hem de granitik sokulumunu kesmektedir. Bu faylar, Kırşehir Masifi'nin Geç Eosen'deki erozyonal yükselimini takiben gelişen ve masifin güney kesiminin yükselimine yol açan Geç Tersiyer yaşlı kıta-kabuğu ölçeğindeki bir gerilmeli tektonizmanın ürünleridir.

Anahtar Sözcükler: Orta Anadolu Kristalen Kompleksi, Hırkadağ, Kırşehir Masifi, Metamorfizma, Termobarometri

Introduction

The Late Mesozoic-Early Cenozoic geologic evolution of the Central Anatolian Crystalline Complex (CACC) involved episodes of deformation, metamorphism, and magmatism associated with contraction and collision along its boundaries. Pressure-temperature paths of metamorphic rocks in the CACC can be used to understand the tectonic history of this region and are useful for comparing different tectonic domains within the CACC.

The high-grade (upper amphibolite facies) section of the Hırkadağ block in the southern Kırşehir Massif of the CACC is particularly interesting because it contains abundant metapelitic rocks with compositions suitable for thermobarometric study. These rocks display reaction textures that record segments of the high-temperature metamorphic P-T path. In addition, the high-angle faults at the boundaries of the block provide evidence for the later tectonic history of the CACC in the vicinity of the Kızılırmak River, the site of a major tectonic discontinuity between the northern and southern CACC (Toprak 1994; Dilek *et al.* 1999).

In this paper, we present results of a study of the highest grade rocks in the Hırkadağ block and discuss the relation of this block to other metamorphic massifs in central Anatolia.

Metamorphic and Tectonic History of the Central Anatolian Crystalline Complex

The Central Anatolian Crystalline Complex is a triangular continental fragment consisting of metamorphic and plutonic rocks (Figure 1); metamorphic rocks are dominantly metasedimentary. Various regions of the CACC have been designated as separate massifs (Kırşehir, Akdağ, Niğde) based on their geographic location. Whitney *et al.* (2001) and Fayon *et al.* (1999a, b) used thermobarometric and thermochronologic data to show that each massif of the CACC had a distinct pressure-temperature-time and tectonic history.

The metamorphic stratigraphy of the massifs can be generalized as follows: (1) The structurally lowest formations consist of upper amphibolite facies metapelitic and semi-pelitic gneiss and schist with interlayered amphibolite, quartzite, marble, and calc-silicate; (2) The overlying, lower grade (amphibolite facies) formations are mostly comprised of calcareous rocks interlayered with schists and amphibolite; and (3) The structurally highest, lowest grade (greenschist to lower amphibolite facies) formation is dominated by calcite marble, with lesser amounts of calc-silicate, quartzite, amphibolite, and fine-grained schist (see Göncüoğlu 1981, 1982, 1986). This general stratigraphy is similar to that described for the '*Cover Series*' of the Menderes Massif in western Turkey (e.g., Dürr *et al.* 1978; Akkök 1983; Şengör *et al.* 1984; Bozkurt & Park 1994).

Every massif in the CACC is intruded by granitoids (e.g., Akıman *et al.* 1993; Erler & Göncüoğlu 1996; Aydın *et al.* 1998; Güleç & Kadıoğlu 1998). Most CACC plutons are Late Cretaceous in age.

The metamorphic and tectonic history of the Kırşehir Massif and other regions of the CACC has been discussed by Erkan (1976, 1978), Seymen (1981), and Whitney *et al.* (2001), and is briefly summarized here. All fission track ages noted are from Fayon *et al.* (1999a, b).

The Kırşehir Block (Kaman area) is characterized by a low to moderate pressure (≤7 kbar) sequence ranging from chlorite to sillimanite-K feldspar zones. An earlier garnet + sillimanite assemblage has been overprinted by cordierite + spinel during high-temperature – low-pressure metamorphism. Apatite fission track ages indicate that the Kırşehir Massif in the vicinity of Kaman was exhumed at or near the Earth's surface by 40 Ma, based on data from two samples of the Baranadağ pluton (one south of Kaman, one to the northeast).

The Akdağ block also ranges from chlorite to sillimanite-K feldspar zones and records moderate pressure (8 kbar) in sillimanite zone rocks containing relict kyanite. Apatite fission track ages from the Ortaköy granite (Figure 1) and a sillimanite-kyanite schist range from 31-35 Ma, but modeling of track length distribution suggests that these Oligocene ages may reflect a re-heating event subsequent to Eocene exhumation.

In contrast to the Kırşehir and Akdağ blocks, the Niğde Massif is a metamorphic core complex. The high-grade core was metamorphosed at 5-6 kbar, 650-700 °C during contraction, exhumed to ~ 10 km by extension, then heated at low pressure by intrusive magmatism (Whitney & Dilek 1997, 1998a, b, 2000). Apatite fission track ages are 9-12 Ma, indicating that the Niğde Massif was exhumed at a much later time than the northern CACC. There is no field evidence or indication in fission

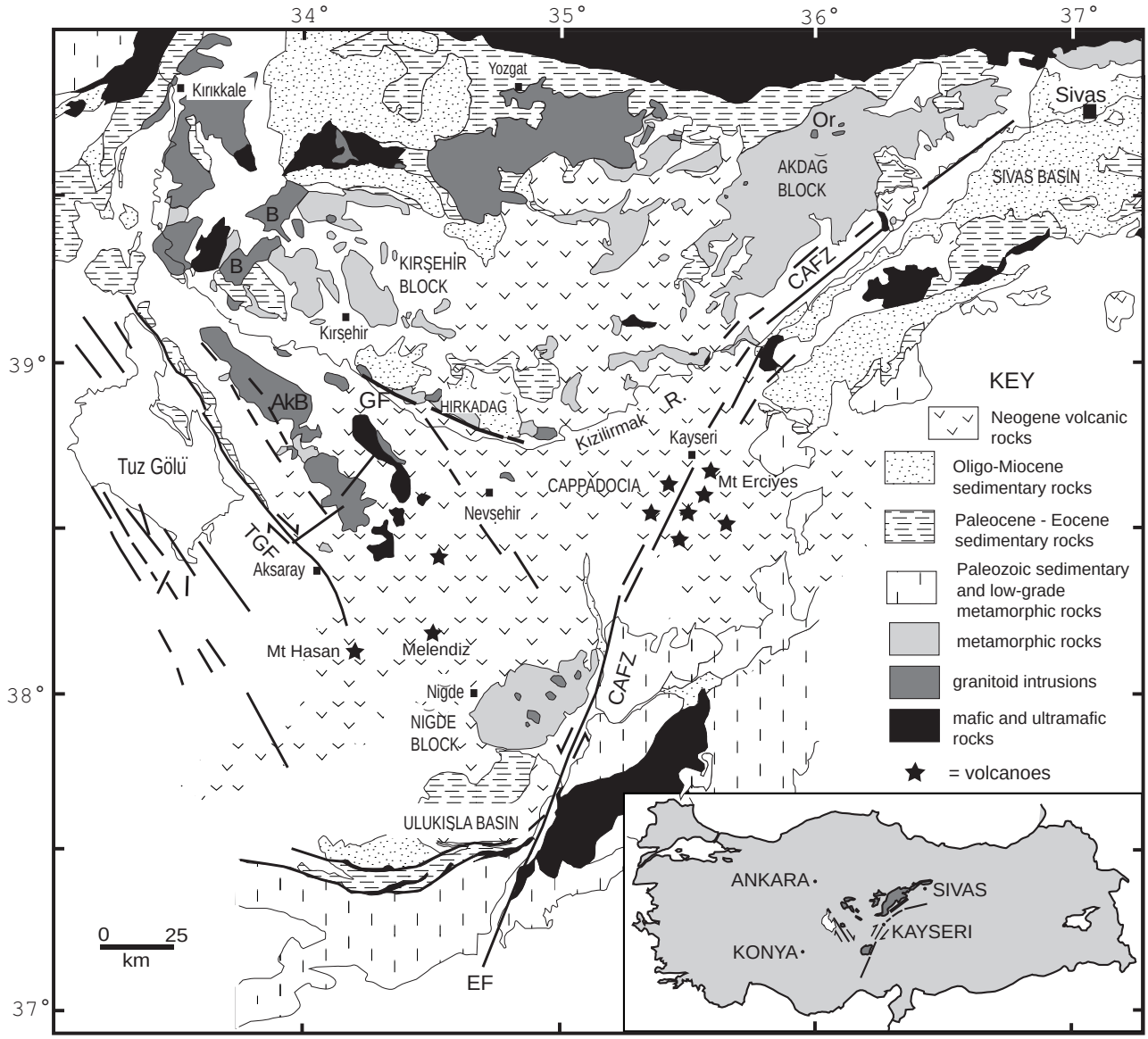

Figure 1. Geologic map of the Central Anatolian Crystalline Complex and vicinity, modified from Erentöz & Ketin (1961). Inset: Map showing the location of the CACC in central Turkey. Key to abbreviations: AkB- Aksaray block; B- Baranadağ pluton; CAFZ- Central Anatolian fault zone; EF- Ecemiş segment of the CAFZ (extends to Kayseri region); GF- Gümüşkent fault; Or- Ortaköy pluton; TGF- Tuz Gölü fault.

track model results for reheating of the Niğde Massif, so these young ages are interpreted to indicate delayed or prolonged unroofing of the Niğde Massif relative to the northern CACC (Whitney *et al.* 2001).

The Aksaray block (Koçak & Leake 1994) is distinct from the other massifs in the CACC in that it is dominated by intrusions; rare metapelitic rocks record low-P (< 4 kbar) regional metamorphism overprinted by low-P – high-T contact metamorphism and partial melting. Low pressure – high temperature metamorphism occurred at shallow mid-crustal levels of an arc, likely associated with magmatism above the subducting Inner Tauride plate. Apatite fission track ages are 45-50 Ma.

These studies have concluded that the northern regions (Kırşehir, Akdağ) experienced thrusting and folding during collision and were slowly exhumed by erosion. Metamorphic rocks are characterized by moderate P/T metamorphism, clockwise P-T paths, and

Eocene-Oligocene apatite fission track ages. In contrast, the southern CACC (Niğde) was metamorphosed in a wrench-dominated setting following collision-related burial and heating. Metamorphic rocks are characterized by clockwise P-T paths followed by low-P – high-T metamorphism, and have Miocene apatite fission track ages (9-12 Ma). Variations in P-T-t and tectonic histories within the CACC reflect the difference between head-on collision (northern CACC) vs. mid-crustal wrenching (Niğde) (Whitney *et al.* 2001).

The Hırkadağ block, in the central part of the CACC, is interesting because it is located near the Kızılırmak River, a tectonic zone (Toprak 1994) that separates the northern vs. southern CACC (Dilek *et al.* 1999). Abundant metapelitic rocks occur in the structurally lowest part of the Hırkadağ block, and these contain unusually large garnets (cm-scale) for the CACC, as well as reaction textures among aluminous phases that allow part of the pressure-temperature path to be reconstructed.

Overview of the Hırkadağ Block

The Hırkadağ block is a NW-SE trending uplift comprised of metamorphic and felsic intrusive rocks, located north of the Kızılırmak River between Gülşehir and Hacıbektaş. This small block is related to the larger Kırşehir Massif to the northwest, but is isolated from the main part of the massif by deformed Oligo-Miocene sedimentary and younger volcanic rocks (Figure 1).

The block is bounded on the northeast and southwest by high-angle normal faults (Figure 2), and by a low-angle fault on the southeast margin. Metamorphic grade ranges from upper amphibolite facies along the southwest margin to greenschist facies along the northeast margin. Lithologies present are similar to other massifs in the CACC: metamorphosed carbonates interlayered with metapelite, quartzite, and amphibolite. The block is intruded by a granitoid pluton that crops out primarily at the eastern end (Figure 2).

The region has been mapped by Atabey (1989), and the petrography and general structure have been described by Aydın (1984) and Teklehaimanot (1993). The samples and field relations we describe here are from the high-grade southwestern margin of the block, with an emphasis on mineral assemblages useful for thermobarometric analysis.

Petrology and Mineral Chemistry

Methods

In the sections below, we describe the mineral assemblages, textures, and compositions for those rocks that were used to estimate pressure-temperature conditions of metamorphism. Thirty-four samples were collected along three approximately NNE-SSW traverses (Figure 2). Mineral compositions from five schists from one traverse were determined with a JEOL JXA-8900 microprobe at the University of Minnesota. Amphibolites collected near the Gülşehir-Hacıbektaş highway were also analyzed. Operating conditions for quantitative analyses (WDS) were 15 kV accelerating voltage, 15-30 nA beam current (lower currents for micas and feldspars, higher currents for garnet), and a range of beam diameters (focused for garnet, defocused to 2-5 mm for micas and feldspars). Natural mineral standards and the ZAF matrix correction routine were used. Representative analyses for minerals from a representative metapelitic schist and amphibolite are given in Tables 1 and 2.

Metapelitic schists

Hırkadağ metapelitic rocks contain large garnets (up to 2 cm in diameter; Figure 3a) + sillimanite + biotite + plagioclase + quartz + potassium feldspar + spinel (hercynite) ± corundum + ilmenite. Some ilmenite grains have thin rims of rutile. Cordierite + sillimanite ± spinel have partially replaced garnet at rims and also occur in patches and along fractures within garnet (Figure 3b). Feldspars and secondary chlorite also commonly occur at resorbed garnet rims (Figure 3a). Schists contain coarse-grained mm- to cm-scale potassium feldspar + quartz-rich layers alternating with finer-grained biotite + plagioclase + sillimanite layers that in some cases lack quartz (Figure 4). Corundum has partially replaced spinel (Figure 4b).

Garnets in metapelitic schist are poikiloblastic (Figure 3a), containing inclusions of plagioclase, quartz, potassium feldspar, ilmenite, spinel, monazite, and allanite. Some inclusions appear texturally late; i.e., they are not former matrix phases enclosed by the growing garnet, but rather grew subsequent to garnet crystallization during partial replacement of garnet by feldspars and cordierite (Figure 3). Garnets are Fe-rich ($Alm_{75-77}Sps_{3-5}Prp_{10-12}Grs_{8-10}$) (Table 1) and display slight growth zoning: cores are richer in Ca and Mn than rims,

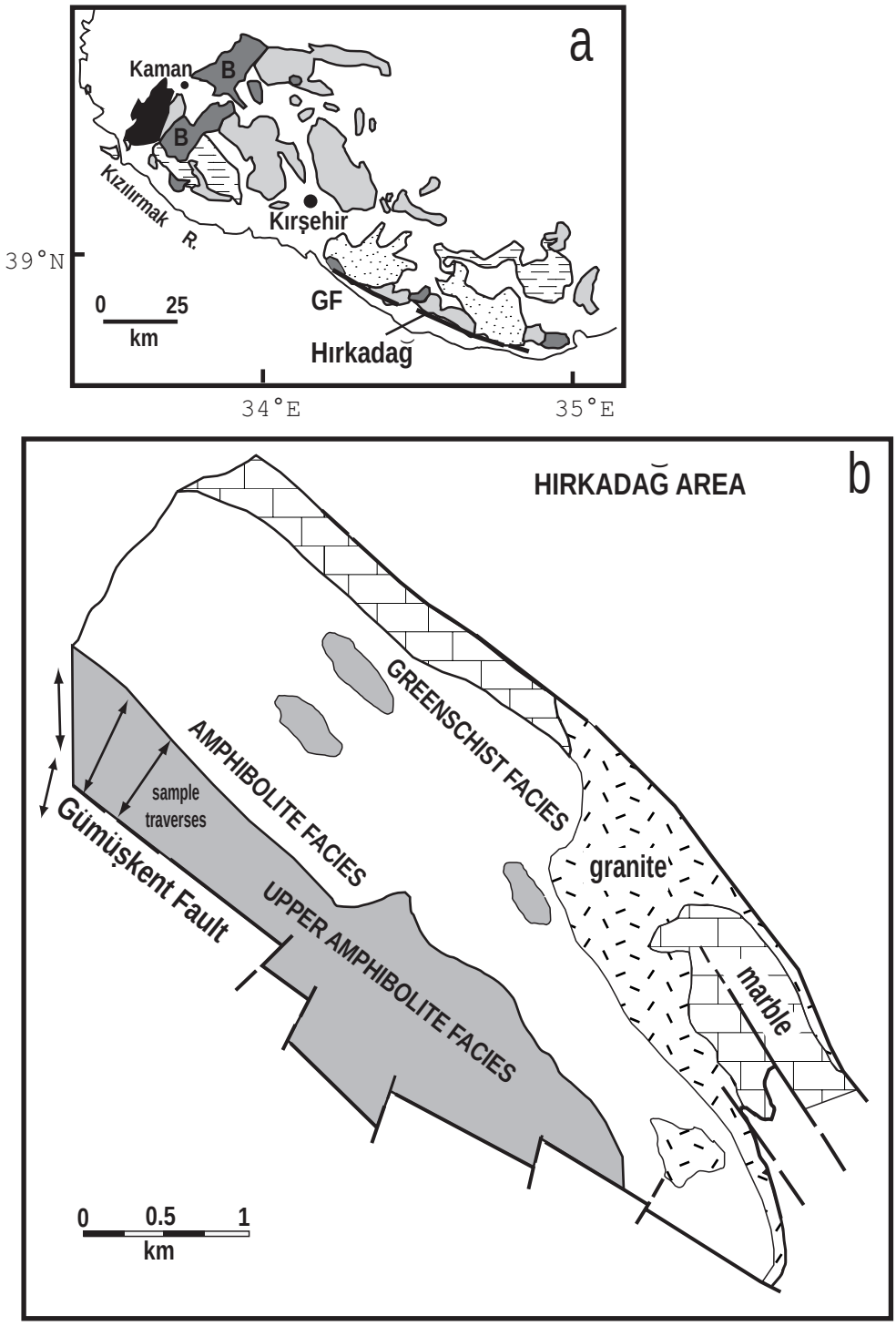

Figure 2. Kırşehir block. **(a)** Geologic map of the northwest region of the CACC; same abbreviations as in Figure 1. **(b)** Geologic map of the SE part of the Hırkadağ region (modified from Teklehaimanot 1993) showing three sampling traverses. All samples discussed in this paper are from the upper amphibolite facies region.

Table 1. Mineral compositions from Hırkadağ garnet-bearing schist.

	KM99-18 Grt rim	KM99-18 Grt core	KM99-18 Bt matrix	KM99-18 Bt pl-layer	KM99-18 Pl rim	KM99-18 Pl rim	KM99-18 Pl core	KM99-18 Pl core	KM99-18 Pl incl	KM99-18 Kfs	KM99-18 Spl*
SiO_2	37.34	37.57	34.92	33.95	65.44	66.72	49.31	56.33	55.30	64.97	< d.l.
TiO_2	0.30	0.31	3.54	5.41	n.a.	n.a.	n.a.	n.a.	n.a.	n.a.	0.06
Al_2O_3	22.14	22.31	17.67	15.40	22.44	20.63	32.20	27.52	28.50	19.49	59.98
FeO	33.15	32.60	19.06	22.88	0.02	0.53	0.09	0.05	0.20	0.03	36.71
MnO	2.05	1.27	< d.l.	< d.l.	n.a.	n.a.	n.a.	n.a.	n.a.	n.a.	< d.l.
MgO	2.47	3.08	9.73	6.94	n.a.	n.a.	n.a.	n.a.	n.a.	n.a.	3.49
CaO	2.63	3.47	0.30	0.17	2.55	0.52	14.41	8.18	10.10	0.11	< d.l.
Na_2O	n.a.	n.a.	0.29	0.35	9.71	10.85	3.39	6.99	5.66	1.45	< d.l.
K_2O	n.a.	n.a.	9.36	9.59	0.02	0.06	0.08	0.17	0.32	13.92	n.a.
total	100.07	100.59	94.86	94.67	100.17	99.31	99.47	99.24	100.08	99.96	100.23
cations											
Si	2.98	2.97	5.36	5.36	2.87	2.94	2.26	2.55	2.49	2.97	
Ti	0.02	0.02	0.41	0.64							
Al	2.09	2.08	3.20	2.87	1.16	1.07	1.74	1.47	1.51	1.05	1.99
Fe	2.21	2.16	2.45	3.02	0.00	0.02	0.00	0.00	0.01	0.00	0.86
Mn	0.14	0.09	0.00	0.00							
Mg	0.29	0.36	2.23	1.63							0.15
Ca	0.23	0.29	0.05	0.03	0.12	0.02	0.71	0.40	0.49	0.01	
Na			0.09	0.11	0.82	0.93	0.30	0.61	0.49	0.13	
K			1.83	1.93	0.00	0.00	0.00	0.01	0.02	0.81	
X_{Alm}	0.77	0.75									
X_{Sps}	0.05	0.03									
X_{Prp}	0.10	0.12									
X_{Grs}	0.08	0.10									
X_{Mg}			0.39	0.29							0.15
X_{An}					0.13	0.03	0.70	0.39	0.49	0.01	
X_{Or}					0.00	0.00	0.00	0.01	0.02	0.86	

* Zn < detection limit in spinel

but contain less Fe. In the vicinity of highly resorbed rims, a thin region of retrograde zoning is observed, characterized by an increase in Mn content of the garnet (~ 3 mol% spessartine higher than core).

Plagioclase inclusions in garnet are typically An_{38-49}, but some grains have patches or rims of nearly pure albite (An_{2-3}), and others are locally as calcic as An_{80}. There does not seem to be a trend in plagioclase composition as a function of inclusion location in garnet (Figure 3a).

Spinel inclusions in garnet are enclosed in plagioclase or cordierite. Inclusion spinel is similar in composition to spinel in the matrix ($Mg^{\#}$ = 14-16), and neither contains much Zn (< 0.1 wt% ZnO). Matrix spinel contains inclusions of sillimanite and potassium feldspar.

Plagioclase-rich domains contain small equant grains of plagioclase associated with randomly oriented, fine-grained biotite + ilmenite + sillimanite + spinel (Figure 4a & c). These plagioclase-rich regions lack quartz, but coarse-grained potassium feldspar adjacent to the plagioclase + biotite domains commonly contains quartz inclusions. The potassium feldspar is slightly zoned, with more Na-rich cores (Table 1). Plagioclase in the plagioclase-rich domains is also zoned, with calcic cores (typically An_{46-63}, locally up to An_{75}) and more sodic rims (An_{12-30}). Biotite is very Ti-rich (4.6-5.7 wt% TiO_2). Spinel occurs as intergrowths with Al_2SiO_5 in quartz-free domains.

Al_2SiO_5 occurs both as prismatic and fibrous sillimanite (Figure 5). In some cases, clusters of relatively coarse

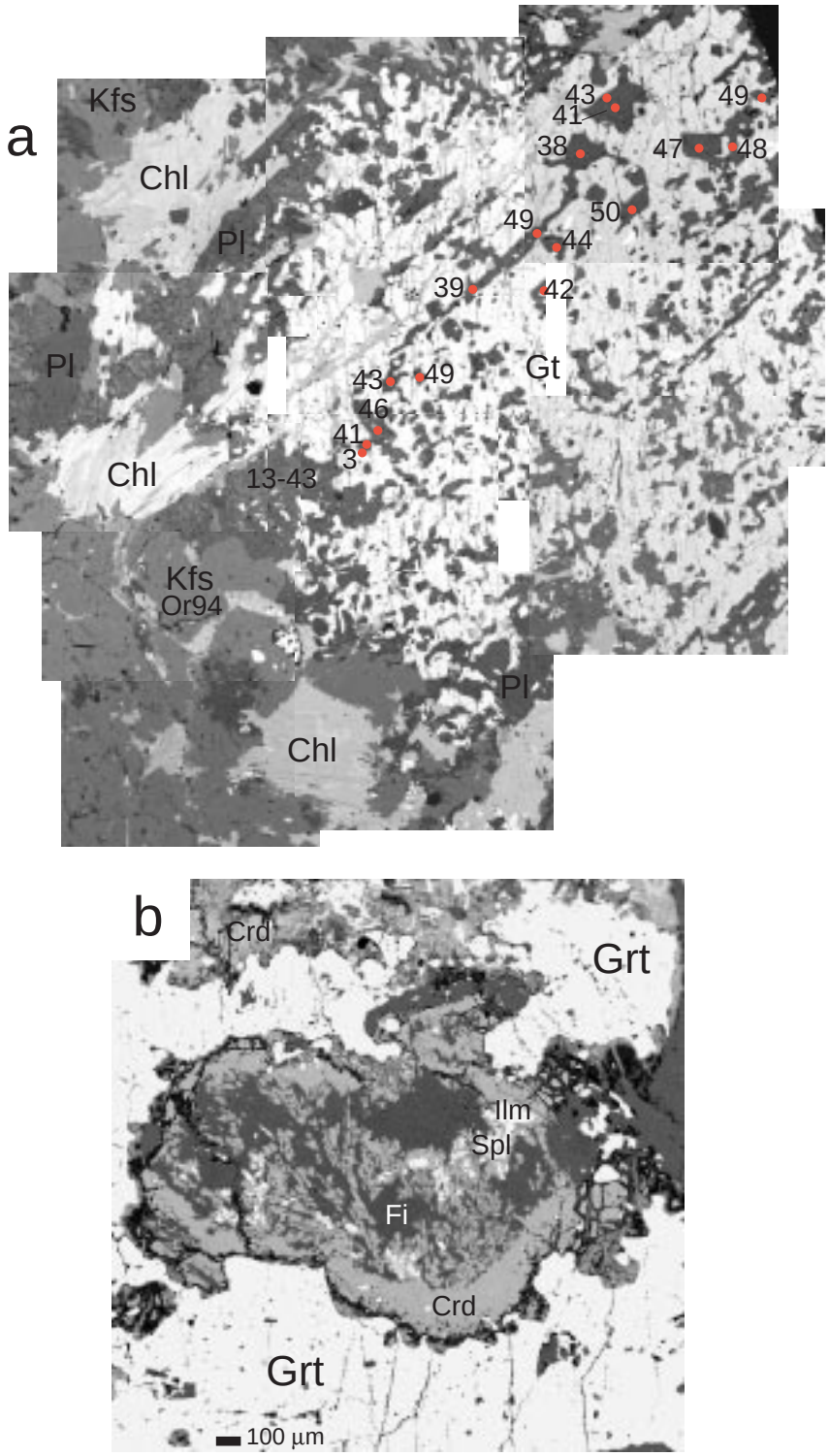

Figure 3. Back-scattered electron (BSE) images of garnet from Hırkadağ metapelitic schist. **(a)** Large poikiloblastic garnet with abundant plagioclase inclusions (anorthite content in mol% shown next to some inclusions). The garnet is ~ 1.5 cm in diameter. **(b)** Patchy replacement of garnet (Grt) by cordierite (Crd) + Sillimanite (Fi-fibrous sillimanite) + Spinel (Spl). Ilm- ilmenite.

Table 2. Mineral compositions from Hırkadağ amphibolite.

	KM99-1d Hbl	KM99-1d Hbl	KM99-1d Hbl	KM99-1d Pl-1	KM99-1d Pl-2	KM99-1d Kfs
SiO_2	48.11	41.58	41.09	48.20	62.06	65.06
TiO_2	0.36	1.84	2.05			n.a.
Al_2O_3	6.49	12.50	13.32	33.35	24.85	18.88
FeO	18.24	18.19	17.89	0.38	0.15	0.24
MnO	0.47	0.41	0.38			n.a.
MgO	11.19	9.17	8.74			n.a.
CaO	12.35	11.62	11.61	15.62	4.71	0.04
Na_2O	1.11	2.15	2.07	2.65	8.84	0.38
K_2O	0.37	1.34	1.27	0.04	0.13	16.12
total	98.69	98.80	98.42	100.24	100.74	100.71
cations						
Si	7.08	6.22	6.16	2.20	2.73	2.98
Ti	0.04	0.21	0.23			
Al	1.13	2.20	2.36	1.80	1.29	1.02
Fe	2.22	2.28	2.25	0.01	0.01	0.01
Mn	0.06	0.05	0.05			
Mg	2.45	2.04	1.95			
Ca	1.95	1.86	1.87	0.76	0.22	0.00
Na	0.32	0.62	0.60	0.23	0.75	0.03
K	0.07	0.26	0.24	0.00	0.01	0.94
X_{Mg}	0.57	0.51	0.50			
X_{An}				0.76	0.23	
X_{Or}						0.96

sillimanite observed in lineation-perpendicular sections appear to have pseudomorphed a tabular mineral, most likely kyanite or andalusite. Although most sillimanite crystals and fibrous mats define a strong lineation, sillimanite crystals oriented at ~ 90° to the dominant direction are common in the metapelitic schists (Figure 5).

Amphibolites

Amphibolites consist primarily of hornblende + plagioclase ± quartz ± biotite, and some contain potassium feldspar as well (Figure 6). Accessory phases are titanite, magnetite, and retrograde chlorite. Some of the amphibolites are fairly massive (not well foliated) and some have fine-scale banding/layering of hornblende and feldspars that defines a foliation.

Plagioclase in the amphibolites is strongly zoned, with An_{52-56} cores and more sodic rims (An_{24-26}). Calcic plagioclase (An_{74}) and potassium feldspar are located at the grain boundaries between plagioclase and hornblende (Figure 6). In some cases, the calcic cores appear euhedral against the sodic rims in BSE images; other grains appear to have more irregular zoning.

Hornblende in the potassium feldspar-bearing amphibolites is relatively rich in K, Na, and Ti: 1.6-2.1 wt% TiO_2, 1.1-2.7 wt% K_2O, 1.6-2.2 wt% Na_2O (Table 2). These amphiboles are similar in mineral chemistry to hornblende in potassium feldspar-bearing amphibolites in the Kaman area of the Kırşehir Massif to the northwest of the Hırkadağ block (Whitney *et al.* 2001). Unlike the Kaman area amphibolites, however, the Hırkadağ amphibolites contain significant amounts of biotite. Some reaction textures suggest that potassium feldspar may have been produced by breakdown of biotite, but Whitney *et al.* (2001) have proposed, based on amphibole chemistry, that some of these rocks represent metamorphosed mafic syenite.

Metacarbonate rocks

Marble and calc-silicate dominate the high-grade zone of the Hırkadağ block, and are even more abundant relative to other rock types in the structurally higher, lower grade parts of the block. Carbonate rocks interlayered with sillimanite-bearing schists contain calcite + quartz + clinopyroxene (diopside) ± scapolite ± plagioclase + titanite. Some calcareous rocks contain wollastonite; both calcite and quartz occur in wollastonite-bearing rocks, although quartz is present in only minor amounts and is typically not in contact with calcite.

Quartzite

Hırkadağ quartzites contain > 95% quartz. Minor phases are muscovite, biotite, Mn-rich garnet, and Fe-oxides. Both quartzites and schists contain highly strained quartz exhibiting a 'chessboard' pattern under crossed polars (Figure 7) indicating the development of both prismatic and basal subgrain boundaries (Kruhl & Huntemann 1991). This extinction pattern has been interpreted as a high temperature (upper amphibolite to granulite facies) feature associated with deformation of β-quartz (Kruhl 1996). At P > 3 kbar, this pattern may indicate deformation temperatures > 650 °C (Figure 8).

Granitoids

The Hırkadağ block is intruded by a granitoid pluton and numerous cm- to meter-scale dikes that range in composition from granite to granodiorite. The main body of the granitoid intrudes all metamorphic units, but

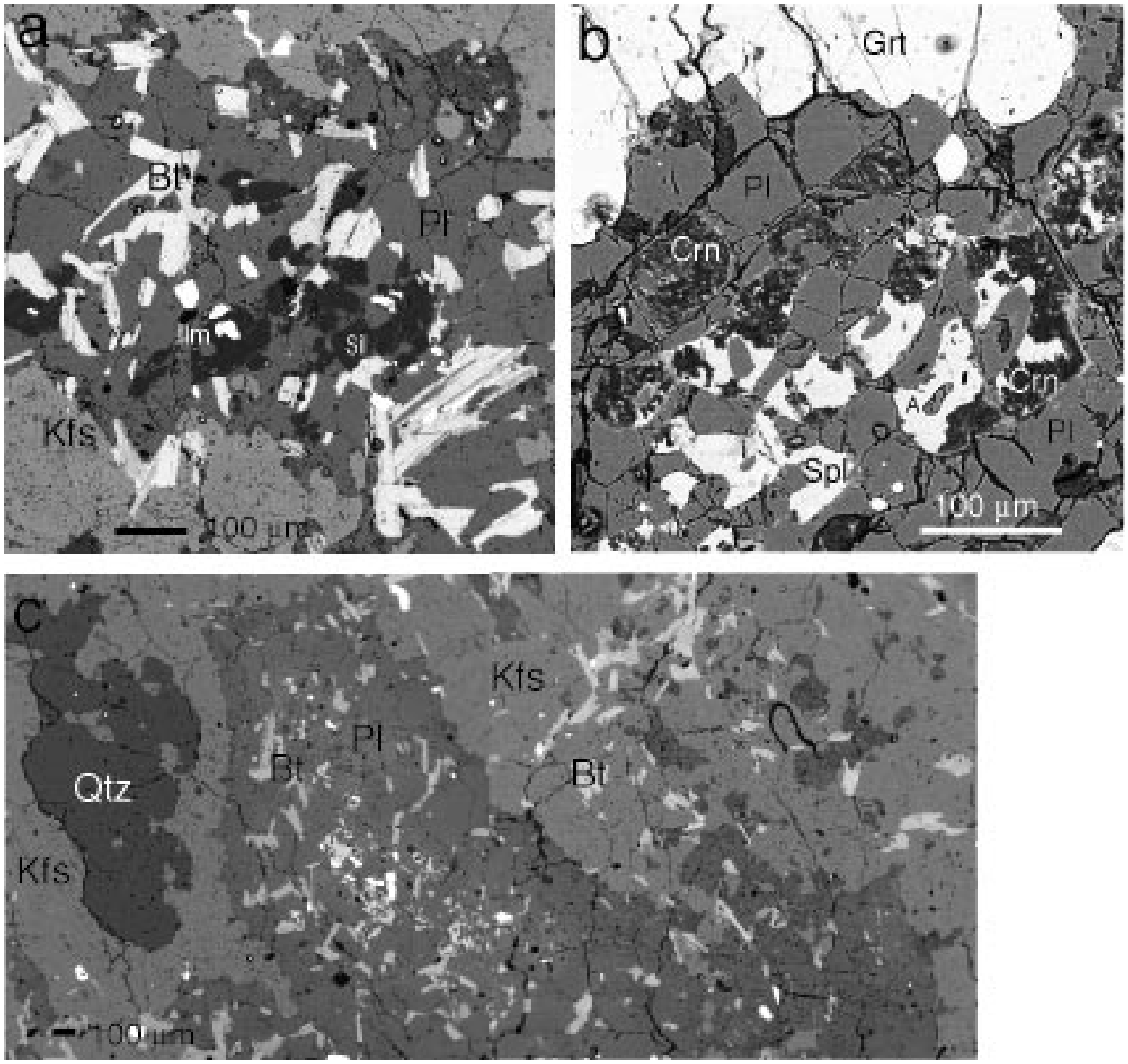

Figure 4. **(a)** BSE image of randomly-oriented biotite + ilmenite + sillimanite in plagioclase-rich, quartz-absent layer in metapelitic schist. **(b)** BSE image of spinel + corundum + plagioclase in garnet. **(c)** Quartz in potassium feldspar (Kfs) layer; the quartz-absent, plagioclase-rich regions are irregular in shape and distribution owing to folding.

mainly crops out in the central and east-southeastern part of the Hırkadağ block (Figure 2b).

Although the contact between the granitoid and the metamorphic country rocks is easily located in the field, it is difficult to determine the nature of the contact because of a highly weathered and fractured zone at the boundary. Most of the metamorphic rocks adjacent to the pluton are marble and thus contact effects are not obvious.

Pressure-Temperature Conditions

Garnet-biotite thermometry results for 5 samples of garnet-sillimanite schist give consistent temperatures of 670-710 °C for garnet compositions just inside the Mn-rich retrograde rim paired with nearby biotite. Garnet-sillimanite-plagioclase-quartz (GASP), garnet-rutile-sillimanite-ilmenite-quartz (GRAIL), and garnet-rutile-ilmenite-plagioclase-quartz (GRIPS) geobarometry yield consistent pressures of 6.6-7.7 kbar (Figure 8).

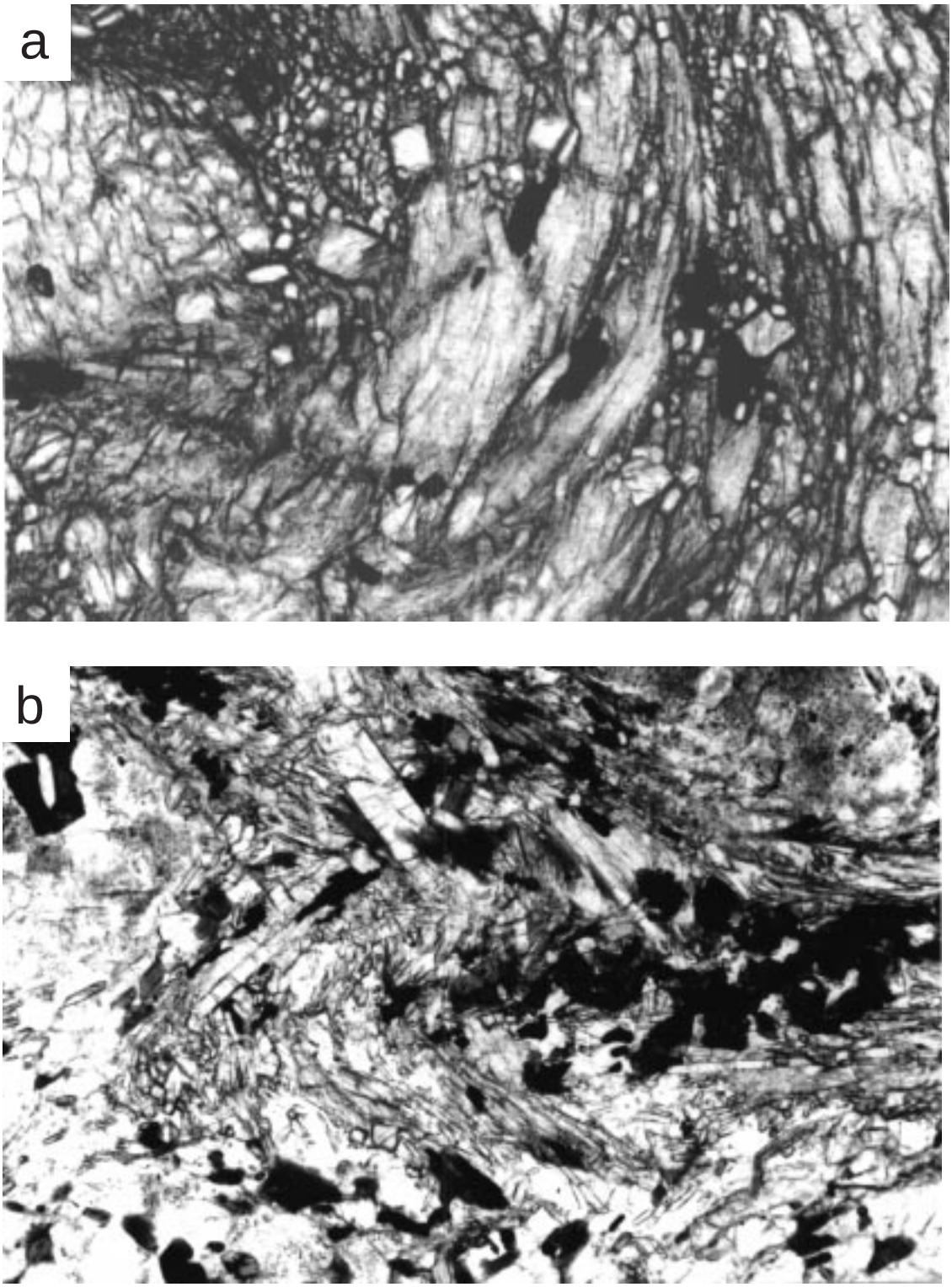

Figure 5. Photomicrographs of sillimanite. **(a)** Prismatic and fibrous sillimanite, including two orientations of prismatic sillimanite at high angles to each other. The fibrous sillimanite is folded in the hinge of a fold. Field of view = 1 mm. **(b)** Two orientations of prismatic sillimanite. Sillimanite crystals outline a fold but are not themselves deformed. The dark minerals are spinel and ilmenite. Field of view = 2 mm.

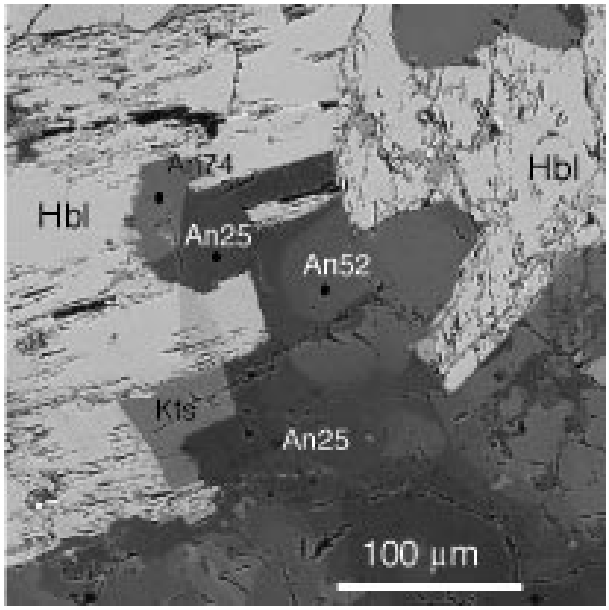

Figure 6. BSE image of Hırkadağ amphibolite. (a) Zoned plagioclase and nearby potassium feldspar in amphibolite.

Amphibolites yield temperatures of 700-770 °C at 4 kbar using the hornblende-plagioclase thermometer (Holland & Blundy 1994). Rims of metapelitic garnets have been resorbed, so these pressure-temperature results may not represent peak conditions, but the homogeneity of garnet, presence of high-temperature mineral inclusions, and correspondence of temperatures between schists and amphibolites suggest that these temperatures may be reasonable estimates of peak conditions.

Garnet-cordierite thermometry yields temperatures of 650-725 °C for cordierite replacing garnet paired with adjacent garnet compositions. Pressures determined from equilibria involving cordierite and spinel in metapelitic rocks are low (3-4 kbar), consistent with these minerals being texturally later than the garnet (Figure 3b). Similar pressures are determined with garnet-cordierite-sillimanite-quartz barometry (3 kbar). Partial replacement of spinel by corundum likely also occurred at high temperatures and low pressures.

No thermobarometric calculations were obtained from rocks to the NE of the high-grade schists and amphibolites. Metamorphic grade decreases to the NE, corresponding to a decrease in structural level (Teklehaimanot 1993). The calc-silicate dominated unit overlying the high-grade schists was metamorphosed in the amphibolite facies, and the marble-dominated unit at

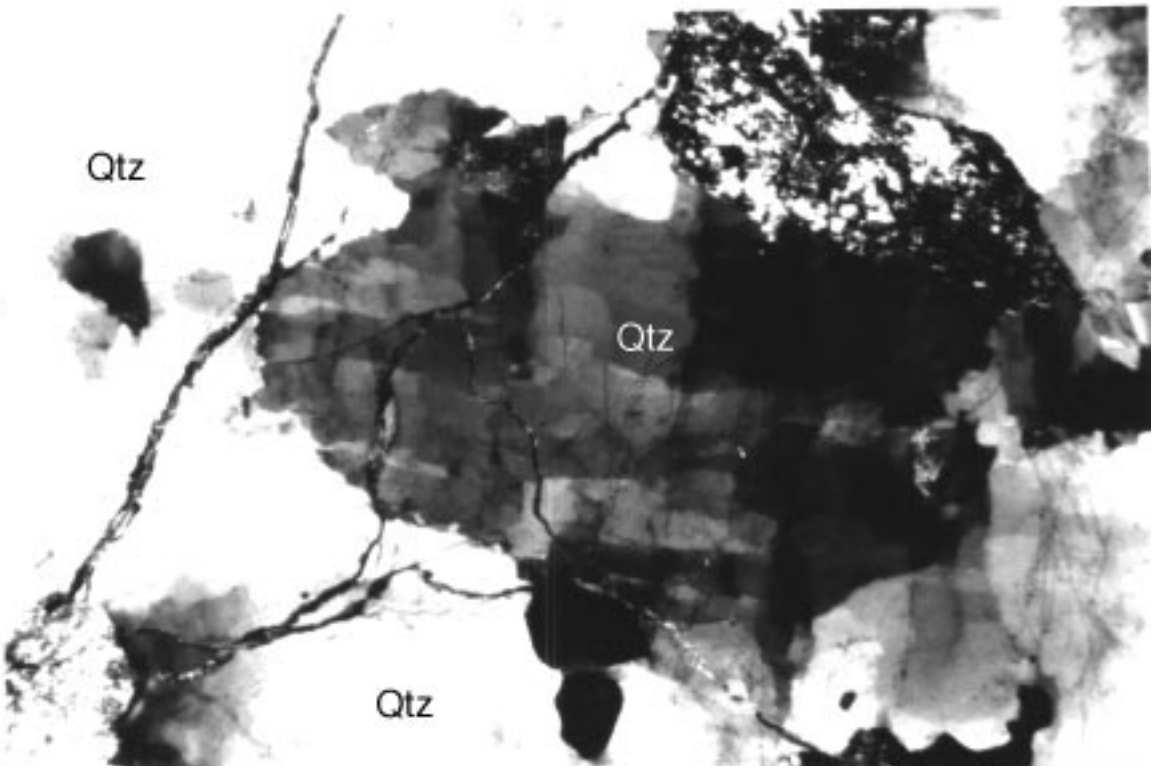

Figure 7. Photomicrograph of quartzite in crossed polarized light showing chessboard extinction in quartz. Field of view = 4 mm.

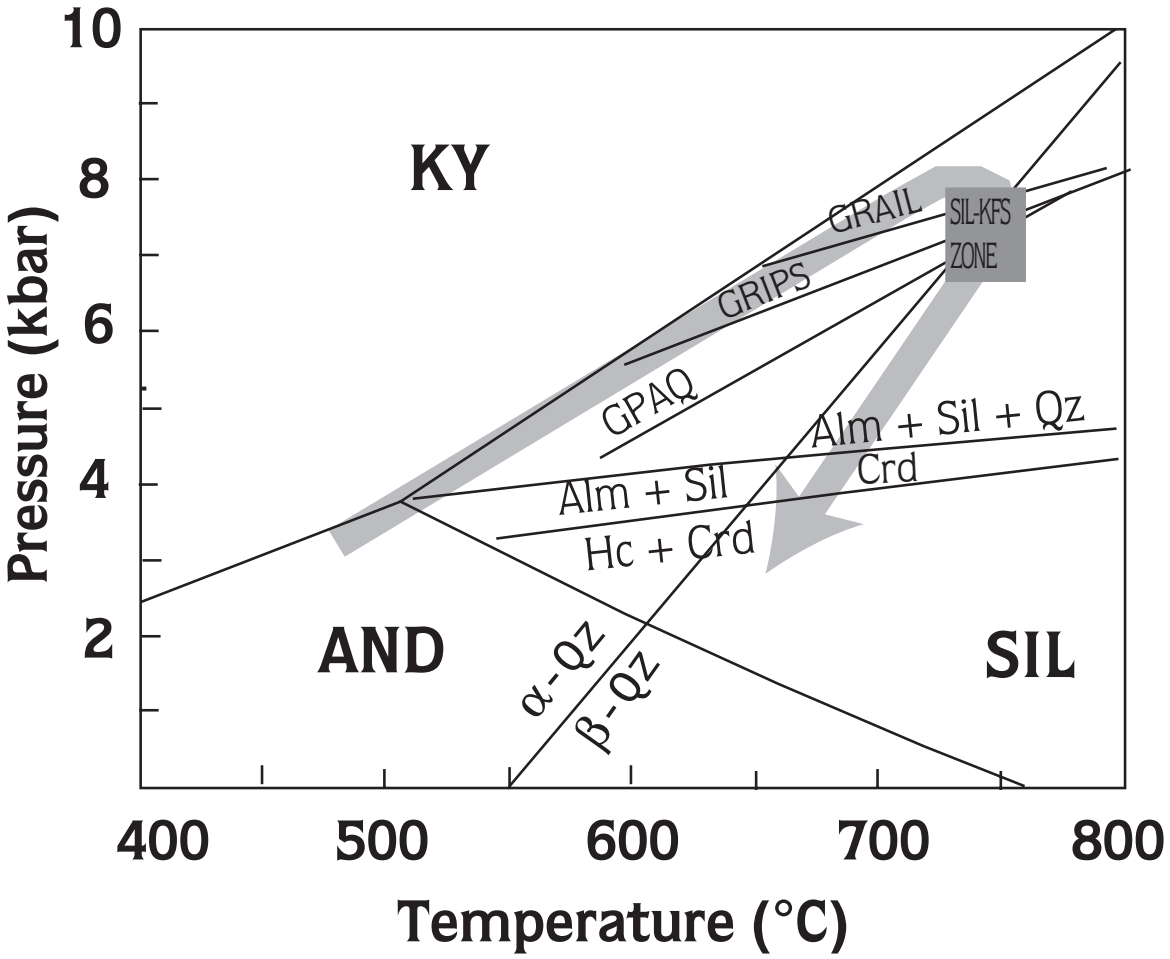

Figure 8. Generalized pressure-temperature path for Hırkadağ metamorphic rocks. The peak of metamorphism is constrained by the intersection of equilibria used as barometers with garnet-biotite equilibria. The high-temperature decompression path was determined from the LP-HT cordierite (Crd) + spinel (Hc, hercynite) assemblage. The prograde path is relatively unconstrained but has been schematically drawn to be consistent with the path inferred from the prograde Barrovian sequence near Kaman (Whitney *et al*. 2001). Alm - almandine; And - andalusite; Ky- kyanite; Qz- quartz; Sil- sillimanite. Baromters: GPAQ- garnet-plagioclase-sillimanite-quartz; GRAIL- garnet-rutile-sillimanite-ilmenite-quartz; GRIPS- garnet-rutile-ilmenite-plagioclase-quartz.

the northeastern margin was metamorphosed in the greenschist to lower amphibolite facies.

Bounding Faults and Adjacent Sedimentary Rocks

The high-angle normal faults along the SW and NE margins of the Hırkadağ block juxtapose metamorphic rocks against sedimentary rocks. Along the SW margin, upper amphibolite facies rocks are in contact with sedimentary rocks along the Gümüşkent fault.

Atabey (1989) mapped the sediments surrounding the Hırkadağ block on the north and south as Oligo-Miocene Yüksekli Formation, described as tuffaceous gravel and sand, sandstone, and red conglomerate. At the southeast end, Atabey (1989) mapped pre-Middle Eocene Saytepe conglomerate. Teklehaimanot (1993) mapped Yüksekli Formation only to the north of the Hırkadağ block, and identified Kızılırmak sediments (Upper Miocene-Pliocene) to the south. We agree with Teklehaimanot (1993) that the sedimentary deposits at the southern margin are Kızılırmak Formation (sandstone, volcanic and volcaniclastic rocks, conglomerate, limestone).

The nature of the contact at the SE end of the Hırkadağ block is, however, problematic. Marble appears to structurally overlie granitoid along a low-angle fault contact, although as noted above, the nature of this contact is difficult to determine. Teklehaimanot (1993) mapped this contact as a thrust fault, consistent with its low angle, and also mapped a thrust contact between the granite and a sedimentary unit. Locally, the presence of blocks in this sedimentary unit is related to a northwest-southeast trending zone of high-angle normal faults that cross-cuts the southeastern margin of the Hırkadağ block, subparallel to the block-bounding faults.

Structure of the Hırkadağ Block

The metapelitic schist and amphibolite interlayered with calc-silicate gneiss display a strong S-C' fabric. The S-surfaces represent the original schistosity resulting from preferred orientation of minerals and/or from lithologic layering. The schistosity planes have a consistent NW attitude with NE and SW dips; they are folded around NW-trending and NW-plunging fold axes. The folds are commonly tight to isoclinal, with overturned southern limbs. They display greater layer thickness in the angular hinge zones than on the limbs, which locally contain parasitic folds. The C-surfaces mark spaced, narrow seams that have NE strikes with NW dips at moderate to gentle angles. The shear indicators along the C-surfaces reveal a top-to-the south reverse displacement, indicating a contractional origin of the S-C fabric. The geometric and kinematic relations between the S-fabric and the NW-plunging folds suggest that the schistosity and folding may be a result of progressive shortening associated with a NNE-SSW-oriented contractional event during and shortly after the peak of metamorphism. The NW-dipping contractional C-fabric in the metamorphic rocks indicates a nearly 90° shift in the orientation of the maximum compressive stress (from NE-SW to NW-SE) subsequent to folding of the original schistosity plane and might have been involved in recrystallization of previously strained mineral grains in the metamorphic rocks. The presence of two directions of sillimanite growth might reflect early alignment as sillimanite grew during development of the main schistosity followed by a second episode of sillimanite growth during low-pressure – high-temperature metamorphism.

NW-striking and variably NE-dipping leucocratic dikes and quartz veins crosscut the S-fabric and the folds in the calc-silicates. Locally, nearly E-W-oriented, subvertical and meter-thick dikes and quartz veins crosscut all fabric elements in the amphibolites. In the quartz veins, quartz crystals that are perpendicular to the vein walls suggest a syntaxial growth mechanism of the formation of these veins due to pure extension in a ~ N-S direction. Evidence for late-stage N-S extension affecting the Hırkadağ metamorphic rocks also includes moderately to steeply S-SW-dipping normal faults in the southwestern part of the block. These show throws of 15 to 20 cm. These faults are subparallel to the Gümüşkent fault, which separates the Hırkadağ block from the Miocene-Pliocene terrestrial deposits of the Kızılırmak Formation.

The high-angle normal faults bounding the Hırkadağ block on the SW and the NE form a NW-SE-trending horst structure. This horst structure is part of a larger, crustal-scale tectonic extension system in the central Kızılırmak River valley that accommodated differential uplift of the southern part of the Kırşehir Massif as well as the adjacent Aksaray block to the south in the Late Tertiary, following their erosional exhumation.

Discussion

Metamorphic Evolution of the Hırkadağ Block

Although geographically isolated from the main body of the Kırşehir Massif (Figures 1 & 2), the Hırkadağ block is similar to the rest of the Kırşehir block in particular and the CACC in general in its metamorphic lithologies and stratigraphy, pressure-temperature conditions and path, its syn-metamorphic structural history, and the relative timing and composition of magmatism. The metapelitic schists and amphibolites along the southwest margin of the Hırkadağ block record $T > 670$ °C at moderate pressure (~ 7 kbar). These are similar conditions to those determined for the high-grade rocks in the Kaman area of the Kırşehir Massif (Whitney *et al.* 2001).

Unique features of the high-grade Hırkadağ metapelitic rocks are the large porphyroblasts (garnet), the occurrence of corundum after spinel, and the segregation of feldspars into distinct alkali feldspar-rich regions and plagioclase-rich regions.

Some of the quartzofeldspathic layers in the metapelitic schists may represent anatectic leucosomes, but the origin of the distinct alkali feldspar + quartz and plagioclase + biotite + sillimanite layers is more

enigmatic. Although the layers themselves are highly deformed (folded), the mineral grains within the layers are typically equant and unstrained, suggesting that some recrystallization occurred subsequent to folding. The K-feldspar + quartz layers are unlikely to represent unmodified leucosomes because they lack plagioclase. The plagioclase + biotite + sillimanite layers also do not appear to be unmodified melanosomes because the biotite is randomly oriented, in contrast to adjacent regions of the schist that contain biotite + sillimanite + plagioclase + quartz + garnet. These layers may represent migmatitic segregations modified by deformation (creating the distinct mineral assemblages in separate layers) and recrystallized during the late low-pressure – high-temperature (LP-HT) event (creating the static texture that has overprinted folding-related deformation).

Petrographic features such as the breakdown of biotite, extensive replacement of garnet by cordierite ± spinel, and the partial replacement of spinel by corundum indicate late, low-pressure – high-temperature metamorphism. LP-HT metamorphic conditions could be attained during high temperature (isothermal) decompression, or could be related to a late thermal event. Similar LP-HT effects are recorded elsewhere in the CACC: in metamorphic rocks north of the Baranadağ granitoid in the Kaman area of the Kırşehir Massif, near the Ortaköy granite in the Akdağ Massif, throughout the Ortaköy region of the Aksaray block, and in the high-grade rocks of the Niğde core complex. LP-HT metamorphism in all of these regions, whether local or widespread, may be related to intrusion of granitic magma. Field relations indicate that magmatic events largely post-dated the peak of regional metamorphism and contractional deformation in each massif.

Tectonic Evolution of the Hırkadağ Block

The development of the main schistosity (S-fabric) in the upper amphibolite facies rocks and the subsequent folding of this schistosity were probably part of the same progressive shortening event. The schistosity likely first developed during the collision of the CACC with the Pontide belt, then was folded during continued shortening in the later stages of collision and contraction. The superimposition of the C-fabric on the earlier-formed schistosity and the attitude of the C-fabric suggest a shift in the orientation of the compressional stress regime. This event may have been associated with the low-pressure – high-temperature event that produced a second generation of oriented, prismatic sillimanite.

The Hırkadağ block is structurally distinct from the rest of the Kırşehir Massif because it is bounded by high-angle normal faults. Field relations show that these faults post-dated metamorphism and likely were not responsible for exhumation of the crystalline rocks in the Hırkadağ block. The block's location at the northern boundary of the Kızılırmak tectonic zone (Toprak 1994) indicates that normal faulting was likely related to extension in this region, perhaps driven by neotectonic escape and rotation of the Anatolian microplate in response to the Miocene-to-present Arabian-Eurasian collision in SE Turkey.

Acknowledgements

This research was supported by NSF grant EAR-9896017 to DLW. We thank M.C. Göncüoğlu, R. Oberhänsli, and A. Okay for helpful reviews, Bülent Teksöz, and Jacquie Smith for assistance in the field in 1999, and M.C. Göncüoğlu for kindly providing a copy of L. Teklehaimanot's thesis.

References

AKIMAN, O., ERLER, A., GÖNCÜOĞLU, M.C., GÜLEÇ, N., GEVEN, A., TÜRELİ, T.K. & KADIOĞLU, Y.K. 1993. Geochemical characteristics of granitoids along the western margin of the Central Anatolian Crystalline Complex and their tectonic implications. *Geological Journal* **28**, 371-382.

AKKÖK, R. 1983. Structural and metamorphic evolution of the northern part of the Menderes massif: new data from the Derbent area and their implications for the tectonics of the massif. *Journal of Geology* **91**, 342-350.

ATABEY, E. 1989. *Kayseri – H19 Paftası Jeoloji Haritası*. General Directorate of Mineral Research and Exploration (MTA) Publication, Ankara, Turkey.

AYDIN, N. 1984. *Orta Anadolu Masifi'nin Gümüşkent B. (Nevşehir) Dolayında Jeolojik – Petrografik İncelemler.* PhD thesis, Ankara University, Ankara, Turkey [in Turkish with English abstract, unpublished].

AYDIN, N., GÖNCÜOĞLU, M.C. & ERLER, E. 1998. Latest Cretaceous magmatism in the Central Anatolian Crystalline Complex: brief review of field, petrographic and geochemical features. *Turkish Journal of Earth Sciences* **7**, 259-268.

BOZKURT, E. & PARK, R.G. 1994. Southern Menderes Massif: an incipient metamorphic core complex in western Anatolia. *Journal of the Geological Society, London* **151**, 213-216.

DILEK, Y., WHITNEY, D.L. & TEKELİ, O. 1999. Links between neotectonic processes and landscape evolution in an Alpine collision zone, south-central Turkey. *Geomorphology* **118**, 147-164.

DÜRR, S. ALTHERR, R., KELLER, J., OKRUSCH, M. & SEIDEL, E. 1978. The Median Aegean Crystalline Belt: stratigraphy, structure, metamorphism, magmatism. *In*: CLOOS, H., ROEDER, D. SCHMIDT, K. (eds.) *Alps, Apennines, Hellenids.* Stuttgart: E. Schweizerbart, 455-477.

ERENTÖZ, C. & KETIN, İ. 1961. *1: 500 000 Scale Türkiye Jeoloji Haritası, Kayseri Sheet.* General Directorate of Mineral Research and Exploration (MTA) Publication, Ankara, Turkey.

ERKAN, Y. 1976. Kırşehir çevresindeki rejyonal metamorfik bölgede saptanan isogradlar ve bunların petrologjik yorumlanmaları. *Yerbilimleri* **2**, 23-54 [in Turkish with English abstract].

ERKAN, Y. 1978. Kırşehir Masifi'nde granat mineralerinin kimyasal bilesimi ile rejyonal metamorfizma arasındaki ilişkiler. *Geological Society of Turkey Bulletin* **21**, 43-50 [in Turkish with English abstract].

ERLER, A. & GÖNCÜOĞLU, M.C. 1996. Geologic and tectonic setting of the Yozgat Batholith, Northern Central Anatolian Crystalline Complex, Turkey. *International Geology Review* **38**, 714-726.

FAYON, A.K., WHITNEY, D.L. & DILEK, Y. 1999a. Constraints on the transition from Alpine crustal thickening to extension in Central Anatolia, Turkey. *EOS* **80**, 1066.

FAYON, A.K., WHITNEY, D.L. & DİLEK, Y. 1999b. Diachronous P-T evolution and differential exhumation within an Alpine microcontinent, Central Anatolia. *Geological Society of America Abstracts with Programs* **31**, 370.

GÖNCÜOĞLU, M.C. 1981. Niğde Masifi'nde viridin-gnaysın kökeni. *Geological Society of Turkey Bulletin* **24**, 45-51 [in Turkish with English abstract].

GÖNCÜOĞLU, M.C. 1982. Niğde Masifi'nde paragnayslarında zirkon U/Pb yaşları. *Geological Society of Turkey Bulletin* **25**, 61-66 [in Turkish with English abstract].

GÖNCÜOĞLU, M.C. 1986. Geochronologic data from the southern part (Niğde area) of the Central Anatolian Massif. *Mineral Research and Exploration Institute of Turkey (MTA) Bulletin* **105/106**, 83-96 [in Turkish with English abstract].

GÜLEÇ, N. & KADIOĞLU, Y.K. 1998. Relative involvement of mantle and crustal components in the Ağaçören granitoid (central Anatolia – Turkey): estimates from trace-element and Sr-isotope data. *Chemie der Erde* **58**, 23-37.

HOLLAND, T.J.B. & BLUNDY, J.D. 1994. Nonideal interactions in calcic amphiboles and their bearing on amphibole-plagioclase thermometry. *Contributions to Mineralogy and Petrology* **116**, 433-447.

KOÇAK, K. & LEAKE, B.E. 1994. The petrology of the Ortaköy district and its ophiolite at the western edge of the Middle Anatolian Massif, Turkey. *Journal of African Earth Sciences* **18**, 163-174.

KRUHL, J.H. 1996. Prism- and basal-plane parallel subgrain boundaries in quartz: a microstructural geothermobarometer. *Journal of Metamorphic Geology* **14**, 581-589.

KRUHL, J.H. & HUNTEMANN, T. 1991. The structural state of the former lower crust in Calabria (S. Italy). *Geologische Rundschau* **80**, 289-302.

ŞENGÖR, A.M.C., SATIR, M. & AKKÖK, R. 1984. Timing of tectonic events in the Menderes massif, western Turkey: implications for tectonic evolution and evidence for Pan-African basement in Turkey. *Tectonics* **3**, 693-707.

SEYMEN, İ. 1981. Kaman (Kırşehir) dolayında Kırşehir Masifi'nin stratigrafisi ve metamorfizması. *Geological Society of Turkey Bulletin* **24**, 101-108 [in Turkish with English abstract].

TEKLEHAIMANOT, L.T. 1993. *Geology and Petrography of Gülşehir Area, Nevşehir, Turkey.* MSc thesis, Middle East Technical University, Ankara, Turkey [unpublished].

TOPRAK, V. 1994. Central Kızılırmak Zone: northern margin of central Anatolian volcanics. *Turkish Journal of Earth Sciences* **3**, 29-38.

WHITNEY, D.L. & DILEK, Y. 1997. Core complex development in central Anatolia. *Geology* **25**, 1023-1026.

Whitney, D.L. & Dilek, Y. 1998a. Metamorphism during crustal thickening and extension in central Anatolia: the Niğde metamorphic core complex. *Journal of Petrology* **39**, 1385-1403.

WHITNEY, D.L. & DİLEK, Y. 1998b. Characterization and interpretation of *P-T* paths with multiple thermal peaks. In: TRELOAR, P.J. & O'BRIEN, P. (eds) *What Drives Metamorphism and Metamorphic Reactions?* Geological Society, London, Special Publications **138**, 47-54.

WHITNEY, D.L. & DILEK, Y. 2000. Andalusite-sillimanite-quartz veins as indicators of low-pressure - high-temperature deformation during late-stage unroofing of a metamorphic core complex, Turkey. *Journal of Metamorphic Geology* **18**, 59-66.

WHITNEY, D.L., TEYSSIER, C., DILEK, Y. & FAYON, A.K. 2001. Influence of orogen-normal collision vs. wrench-dominated tectonics on metamorphic P-T-t paths, Central Anatolia Crystalline Complex, Turkey. *Journal of Metamorphic Geology* (in press).